Hindered Transport of Macromolecules in Isolated Glomeruli. II. Convection and Pressure Effects in Basement Membrane

Aurélie Edwards,* Barbara S. Daniels,# and William M. Deen*
*Department of Chemical Engineering, Massachusetts Institute of Technology, Cambridge, Massachusetts 02139, and #Department of Medicine, University of Minnesota, Minneapolis, Minnesota 55455 USA

ABSTRACT The filtration rates for water and a polydisperse mixture of Ficoll across films of isolated glomerular basement membrane (GBM) were measured to characterize convective transport across this part of the glomerular capillary wall. Glomeruli were isolated from rat kidneys and the cells were removed by detergent lysis, leaving a preparation containing almost pure GBM that could be consolidated into a layer at the base of a small ultrafiltration cell. A Ficoll mixture with Stokes-Einstein radii ranging from about 2.0 to 7.0 nm was labeled with fluorescein, providing a set of rigid, spherical test macromolecules with little molecular charge. Filtration experiments were performed at two physiologically relevant hydraulic pressure differences (ΔP), 35 and 60 mmHg. The sieving coefficient (filtrate-to-retentate concentration ratio) for a given size of Ficoll tended to be larger at 35 than at 60 mmHg, the changes being greater for the smaller molecules. The Darcy permeability also varied inversely with pressure, averaging 1.48 ± 0.10 nm^2 at 35 mmHg and 0.82 ± 0.07 nm^2 at 60 mmHg. Both effects could be explained most simply by postulating that the intrinsic permeability properties of the GBM change in response to compression. The sieving data were consistent with linear declines in the hindrance factors for convection and diffusion with increasing pressure, and correlations were derived to relate those hindrance factors to molecular size and ΔP. Comparisons with previous Ficoll sieving data for rats in vivo suggest that the GBM is less size-restrictive than the cell layers, but that its contribution to the overall size selectivity of the barrier is not negligible. Theoretical predictions of the Darcy permeability based on a model in which the GBM is a random fibrous network consisting of two populations of fibers were in excellent agreement with the present data and with ultrastructural observations in the literature.

INTRODUCTION

The renal glomerular capillaries are highly permeable to water, yet very restrictive to the major plasma proteins, thereby permitting formation of the large volume of nearly protein-free ultrafiltrate required for normal kidney function. An important component of the filtration barrier is the glomerular basement membrane (GBM), a fibrous, gel-like structure that is interposed between endothelial and epithelial cell layers. Characterizing the permeability properties of the GBM is necessary for understanding normal barrier function and for gaining insight into the changes that occur when glomeruli are injured by disease. Two approaches have been used to study the hydraulic and/or macromolecular permeability of GBM. Isolated basement membrane can be compressed in a filtration cell (Daniels et al., 1992, 1993; Daniels, 1994; Robinson and Walton, 1987, 1989; Walton et al., 1992), a pressure applied, and filtration rates measured for water and various test macromolecules, such as albumin and dextran. The sieving coefficient (Θ) of a macromolecule is the filtrate-to-retentate concentration ratio. An alternative approach has been to measure diffusion of fluorescent macromolecules across the walls of optical cross sections of single capillary loops of isolated glomeruli with a confocal microscopy technique (Daniels et al., 1993; Edwards et al., 1997). This has been done both with intact glomeruli and with glomeruli in which the cells were removed by detergent lysis; the cell-free glomeruli consist essentially of GBM skeletons, which maintain the general shape of the glomerulus. Thus both the hydraulic permeability of GBM and the convective and/or diffusive transport rates of certain macromolecules can be determined in vitro.

As a first approximation, GBM may be modeled as an isotropic material in which the flux N of a macromolecule is the sum of two terms, a diffusive and a convective component. The total flux is written as

$$N = -K_d D_\infty \nabla C + K_c \nu C, \quad (1)$$

where C is the volume-averaged solute concentration at any point in the GBM, D_∞ is the solute diffusivity in bulk solution, and ν is the volume-averaged or superficial velocity (volume flux). The dimensionless coefficients K_d and K_c describe hindrances to diffusion and convection, respectively. The diffusivity of the macromolecule within the membrane is $K_d D_\infty$, and the apparent velocity for convective transport is $K_c \nu$. The hindrance coefficients depend on molecular size, shape, and perhaps also molecular charge. In general, steric and hydrodynamic interactions between the membrane and a molecule of finite size will cause both K_d and K_c to be less than unity.

In the companion study (Edwards et al., 1997) we used the confocal microscopy technique to measure rates of diffusion of Ficoll across isolated GBM. Ficoll, a cross-

Received for publication 1 April 1996 and in final form 2 October 1996.
Address reprint requests to Dr. William M. Deen, Department of Chemical Engineering, Room 66-509, Massachusetts Institute of Technology, 77 Massachusetts Avenue, Cambridge, MA 02139-4307. Tel.: 617-253-4535; Fax: 617-258-8224; E-mail: wmdeen@mit.edu.

0006-3495/97/01/214/09 $2.00

linked copolymer of sucrose and epichlorohydrin, appears to be a nearly ideal probe for investigating molecular size effects because it behaves much like a neutral, rigid sphere (Davidson and Deen, 1988). Integrating Eq. 1 across a layer of GBM of thickness δ, under steady or pseudo-steady conditions, gives

$$N = \frac{\Phi K_d D_\infty}{\delta} \Delta C \equiv k_{bare} \Delta C, \quad (2)$$

where Φ is the partition coefficient (ratio of membrane to external solute concentration at equilibrium), ΔC is the concentration difference between the external solutions, and k_{bare} is the solute permeabilty of the bare GBM. Thus with D_∞ and δ known, measurements of k_{bare} allowed us to evaluate the product, ΦK_d, as a function of the Stokes-Einstein radius of Ficoll (Edwards et al., 1997). The objective of the present study was to use the filtration method to evaluate ΦK_c for Ficoll, thereby providing a more complete description of size-based hindrances to transport in the GBM.

The rationale for the present experimental design is seen by integrating Eq. 1 across the thickness of the barrier, under conditions of steady (or pseudo-steady) filtration. The result for the sieving coefficient is

$$\Theta = \frac{\Phi K_c}{1 - (1 - \Phi K_c)\exp(-\mathrm{Pe})} \quad (3)$$

$$\mathrm{Pe} = \frac{(\Phi K_c) v \delta}{(\Phi K_d) D_\infty}, \quad (4)$$

where Pe is the membrane Peclet number (which measures the importance of convection relative to diffusion). The common factor Φ has been retained in Eq. 4 to emphasize that experiments interpreted using Eqs. 2 and 3 yield only the products ΦK_d and ΦK_c, and not the hindrance factors alone. The experiments were designed to exploit the expected inverse relationship between the sieving coefficient and Peclet number shown by Eq. 3. That relationship is illustrated in Fig. 1, which shows sieving coefficients predicted for two different filtration velocities. Decreases in v tend to increase Θ, the changes being more pronounced for smaller macromolecules. The increase in Θ for lowered v (smaller Pe) is due to the greater opportunity for diffusional equilibration between filtrate and retentate; no effect of v is expected for very large molecules, where the diffusive part of the flux is negligible. Although Fig. 1 is based on coefficients calculated for a hypothetical membrane containing uniform cylindrical pores, the same qualitative effect of v is expected for other structures. Thus we measured Ficoll sieving coefficients as a function of molecular size at two applied pressures, so that for each Ficoll size there would be two data points that could be used (in principle) to calculate the two unknowns, ΦK_d and ΦK_c. As will be discussed, the actual findings were more complicated to interpret, because of the effects of pressure on the properties of the GBM.

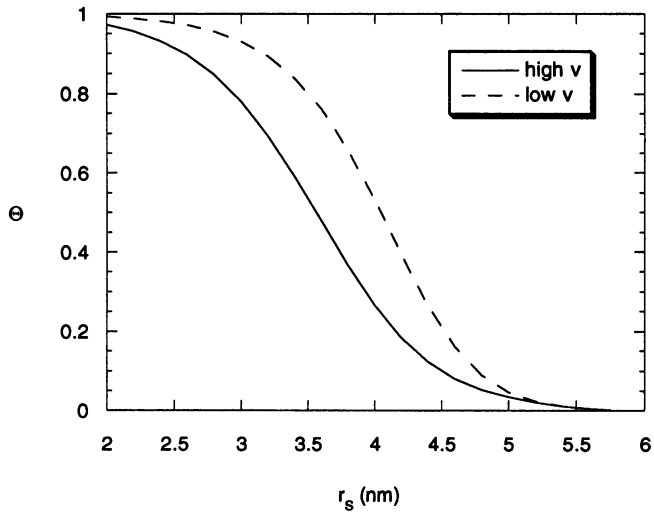

FIGURE 1 Predicted effects of volume flux (v) on sieving coefficient (Θ), as a function of Stokes-Einstein radius (r_s). The calculations are based on a theory for uncharged, spherical macromolecules in uniform cylindrical pores (Maddox et al., 1992). The pore radius and pore length were assumed to be 6.0 nm and 6.0 μm, respectively. The "low" and "high" volume fluxes correspond to 0.75×10^{-7} and 3×10^{-7} m/s, respectively.

MATERIALS AND METHODS

Preparation of isolated GBM

Glomeruli were isolated from Sprague-Dawley rats, and detergent lysis was used to remove the cells, as described previously (Daniels et al., 1992). The resulting glomerular skeletons maintained the general shape of the glomerulus and were composed predominantly of GBM, with a few areas of residual mesangial matrix. Immunofluorescence microscopy of GBM obtained in that manner shows the presence of laminin, type IV collagen, and heparan sulfate proteoglycan (Daniels et al., 1992).

Macromolecules

The ultrafiltration experiments were performed using a polydisperse preparation of Ficoll with a weight-averaged molecular weight of 70,000 (Ficoll 70; Pharmacia, Piscataway, NJ). The Ficoll was labeled with DTAF (dichlorotryazinyl amino fluorescein) (Sigma Chemical Co., St. Louis, MO) using a procedure described by De Belder and Granath (1973). Samples were purified from unreacted label using desalting columns (Bio-Rad, Hercules, CA) and freeze-dried until used. The number of fluoresceins per Ficoll molecule was estimated to be less than three, so that the negative charge due to fluorescein was assumed to be negligible. Four narrow fractions of fluorescein-Ficoll, characterized previously (Johnson et al., 1996), were used for calibration of the gel chromatography column (see below).

Ultrafiltration experiments

The acellular glomeruli were consolidated in a modified mini-ultrafiltration cell (model 3; Amicon, Beverly, MA) as described previously (Daniels et al., 1992). Briefly, 150 μg of GBM suspended in Krebs-bicarbonate buffer (pH 7.4) was added to the cell. Stirring was initiated, and 1500 mmHg of pressure, generated with compressed air, was applied for 1 h to pack the GBM into a homogeneous layer on a piece of filter paper. The resulting layers of GBM appeared uniform by light microscopy and were impermeable to blue dextran (molecular weight of 10^6) (Daniels et al., 1992). After consolidation, the buffer was removed and replaced with identical buffer

containing 4 g/dl bovine serum albumin (BSA) and 0.05 g/dl of the polydisperse fluorescein-Ficoll. Filtration studies were performed at 27°C, with an applied pressure of either 35 or 60 mmHg and a stirring rate of 220 rpm. After a 10-min equilibration period, the filtrate was collected for 1 h. The volume of filtrate was measured for calculation of the hydraulic permeability. The filtrate, and retentate samples taken at the start and end of the collection period, were subjected to gel chromatography for determination of sieving coefficients as a function of molecular size (see below). The concentration of BSA in the filtrate was determined for calculation of its sieving coefficient.

Darcy permeability

The hydraulic permeability (L_p) of the GBM filters is related to v by

$$v = L_p(\Delta P - \sigma_{BSA}\Delta\Pi_{BSA}), \quad (5)$$

where σ_{BSA} and $\Delta\Pi_{BSA}$ are the reflection coefficient and osmotic pressure difference, respectively, for albumin. The reflection coefficient was estimated as $1 - \Theta_{BSA}$, and the osmotic pressures were calculated using the correlation given by Vilker et al. (1981). The retentate concentration was corrected for concentration polarization, as described below. Together with the measured values of v and ΔP, this information permitted the calculation of L_p for each run. The Darcy permeability of the GBM (κ) was then obtained as

$$\kappa = \mu L_p \delta, \quad (6)$$

where μ is the viscosity of water at 27°C. The thickness of the packed layer of GBM (δ) was determined after the completion of each filtration experiment by morphometric techniques (Daniels et al., 1992).

Sieving coefficients

Filtrate and retentate samples were chromatographed on columns of 2.6 cm diameter (model C 26/100; Pharmacia) packed with Sephacryl S-300 HR (Pharmacia). The eluent buffer was 0.05 M ammonium acetate at pH 7.0. Continuous Ficoll elution curves were determined by fluorescence spectrophotometry (model RF-551; Shimadzu, Columbia, MD). The void volume of the column was determined by the elution of fluorescein isothiocyanate dextran (FITC-dextran, 2×10^6 MW; Sigma). Four narrow fractions of fluorescein-labeled Ficoll of known Stokes-Einstein radius (r_s = 3.0, 3.8, 4.8, and 6.2 nm) were used to calibrate the column.

Concentration polarization causes the solute concentration at the membrane surface (C_M) to exceed that in the bulk retentate (C_R). Accordingly, the measured sieving coefficient ($\Theta' = C_F/C_R$, where C_F is the filtrate concentration) is larger than the true sieving coefficient for the membrane ($\Theta = C_F/C_M$). The relationship between Θ and Θ' is

$$\Theta = \frac{\Theta'}{(1 - \Theta')\exp(v/k_c) + \Theta'}, \quad (7)$$

where k_c is the mass transfer coefficient in the retentate. In our previous studies (Daniels et al., 1992, 1993; Daniels, 1994) the value of k_c was calculated from a correlation in the literature. To obtain a more accurate value for our particular apparatus, a separate set of experiments was performed to measure the mass transfer coefficient, as detailed in the Appendix.

RESULTS

Darcy permeability

The results for water flow and membrane thickness are shown in Table 1. As expected, the filtrate velocity was much larger at the higher pressure. Although the experiments were performed in random order and all involved approximately the same amounts of GBM, the membrane thickness (δ_0) measured after the experiment was ~30% larger, on average, for those at ΔP = 35 mmHg than for those at ΔP = 60 mmHg. The samples were fixed for morphometry after the pressure in the cell was released, so that we assume that all measured thicknesses correspond to $\Delta P = 0$, rather than the actual pressure used in the filtration experiment. Thus it appears that the difference in δ_0 between the two groups of experiments is coincidental. To estimate the corresponding thicknesses under compression, we used results obtained by Walton et al. (1992). Reported in their study were measurements of δ for a wide range of pressures, from which we derived a relationship between the deformation of GBM filters and the applied pressure. We estimate that δ/δ_0 was 0.94 at 35 mmHg and 0.90 at 60 mmHg; the corresponding values of δ are shown in Table 1.

TABLE 1 Flow rate, membrane thickness, and water permeability

	ΔP = 35 mmHg	ΔP = 60 mmHg
v (10^{-7} m/s)	6.26 ± 0.44	9.34 ± 0.38*
δ_0 (μm)	7.77 ± 0.69	6.02 ± 0.49
δ (μm)	7.29 ± 0.65	5.42 ± 0.44*
L_p (10^{-8} m/s/mmHg)	3.29 ± 0.29	2.37 ± 0.13*
κ (nm^2)	1.48 ± 0.10	0.82 ± 0.07*

Results are given as mean ± SE for n = 6.
*$p < 0.05$ versus 35 mmHg.

As shown in Table 1, the hydraulic permeability (L_p) was found to be about 40% larger at ΔP = 35 mmHg than at ΔP = 60 mmHg, despite the differences in membrane thickness. That is, because L_p is inversely proportional to membrane thickness (all else being equal), the differences in δ (or δ_0) alone would have led to a lower, not a higher, value of L_p at the lower pressure. The Darcy permeability, a measure of fluid permeability that is independent of the sample thickness, was found to equal 1.48 ± 0.10 nm^2 (n = 6) at 35 mmHg and 0.82 ± 0.07 nm^2 (n = 6) at 60 mmHg (Table 1). Thus we conclude from the results in Table 1 that the difference in pressure led to a difference in the intrinsic permeability properties of the GBM to water and (presumably) to macromolecules. Decreases in L_p with increasing pressure have also been observed previously with isolated GBM (Robinson and Walton, 1989; Walton et al., 1992; Daniels et al., 1992).

Sieving curves

The measured sieving coefficients for Ficoll are shown by the individual symbols in Fig. 2. At either pressure, Θ decreased gradually with increases in molecular size. For any given molecular size Θ was elevated at the lower pressure, where v was smaller, and this effect was most pronounced for the smaller Ficoll molecules. Thus the measured sieving coefficients were qualitatively consistent with the expectations from Fig. 1. However, the underlying

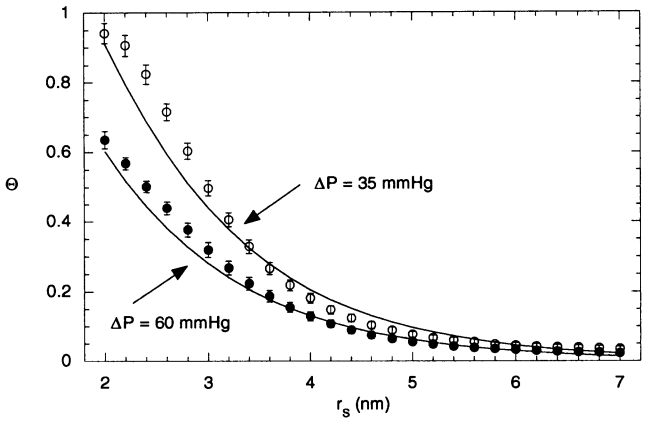

FIGURE 2 Ficoll sieving coefficients measured for isolated GBM at two applied pressures. Results are given as mean ± SE, with $n = 6$ in both cases. The curves are based on Eqs. 3 and 8–10.

mechanism for the shift in the sieving curves is not what we had anticipated. Unlike the situation in Fig. 1, the change in filtrate velocity corresponded to little or no change in Pe for any given molecular size. This is indicated by the product $\nu\delta$, which appears in the numerator of Eq. 4. The average values of $\nu\delta$ were 5.05 ± 0.41 ($\times 10^{-12}$ m^2/s) for $\Delta P = 60$ mmHg and 4.46 ± 0.26 ($\times$ 10^{-12} m^2/s) for $\Delta P = 35$ mmHg, which are not statistically different. We conclude that the differences in the two sets of sieving coefficients are attributable mainly to the fact that the permeability properties of the GBM depend on the applied pressure, and not to changes in Pe. The curves shown in Fig. 2, which represent fits to the data, are discussed later.

Hindrance coefficients

Based mainly on the findings in Table 1, the assumption that ΦK_d and ΦK_c are constants for a given size of Ficoll does not seem viable. Instead it is necessary to account for the probable dependence of ΦK_d and ΦK_c on ΔP. As the GBM is compressed, increasing the concentration of collagen IV and other fibrous solids, steric and hydrodynamic restrictions on the movement of macromolecules will tend to be increased. Accordingly, we expect both ΦK_d and ΦK_c to decrease with increasing pressure. For simplicity, we assumed that both relationships were linear. Calculations based on a recent model for hindered diffusion of macromolecules in random arrays of fibers (Johnson et al., 1996) indeed suggest an approximate linearity between ΦK_d and ΔP; these calculations are discussed in Edwards (1996).

The quantity ΦK_d was determined for $\Delta P = 0$ in the companion paper (Edwards et al., 1997). The results for Ficoll sizes ranging from 3.0 to 6.2 nm were represented by

$$(\Phi K_d)_0 = 0.1045 \exp(-0.7302 r_s), \quad (8)$$

where r_s is in nanometers and the subcript 0 indicates that this expression is for $\Delta P = 0$. To extrapolate those results to the present conditions ($\Delta P = 35$ and 60 mmHg), we assumed that

$$\frac{(\Phi K_d)}{(\Phi K_d)_0} = 1 - \beta \Delta P = \frac{(\Phi K_c)}{(\Phi K_c)_0}, \quad (9)$$

where β is a positive constant. As indicated by the second equality in Eq. 9, we assumed that the factor for convection depended on ΔP in the same manner as that for diffusion.

Equation 9 contains two unknown parameters for each solute size, β and $(\Phi K_c)_0$. To assess the utility of that relationship, those parameters were evaluated first for each size of Ficoll, using Eq. 3 and the sieving coefficients measured at the two pressures. The dependence of β on solute size was found to be very weak, so that we assumed subsequently that β was constant for all r_s. When we allowed β for convection to differ from that for diffusion, very similar values were obtained, and there was not a significant improvement in the fit to the sieving data. Overall, assuming that $\beta = 0.0096$ mmHg^{-1} for all solute sizes, for both convection and diffusion, led to very satisfactory results. The values of $(\Phi K_c)_0$ calculated using these assumptions were represented well by

$$(\Phi K_c)_0 = 6.0240 \exp(-0.7469 r_s), \quad (10)$$

where r_s is in nanometers. Equations 3 and 8–10, with the aforementioned value of β, provided very good fits to the sieving data. The sieving coefficients calculated in this manner are shown by the curves in Fig. 2. Thus the empiricism represented by Eq. 9 was found to be very effective.

Plotted in Fig. 3 are $(\Phi K_d)_0$ and $(\Phi K_c)_0$ as a function of solute radius, as given by Eqs. 8 and 10. Both quantities are seen to decrease monotonically with increases in r_s. The hindrances to convective movement of Ficoll were found to be much less severe than those for diffusion. That is, for the entire range of molecular sizes studied, $(\Phi K_c)_0$ greatly ex-

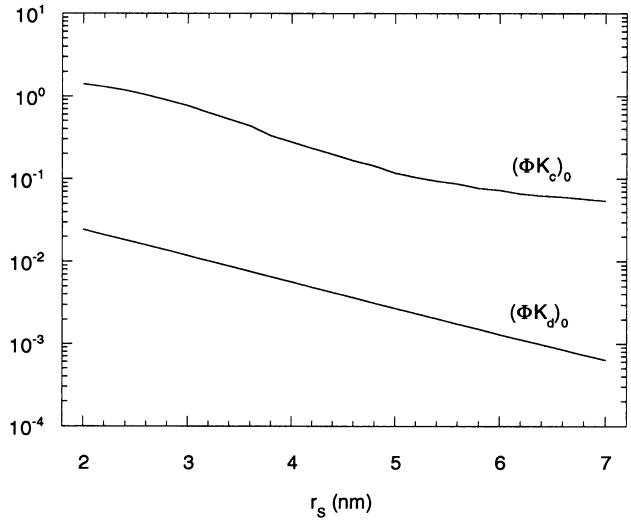

FIGURE 3 Hindrance coefficients in the GBM as a function of molecular size. The values shown are for zero applied pressure.

ceeded $(\Phi K_d)_0$. The ratio of these quantities was $\sim 10^2$ for all r_s. Note that, because Eq. 8 is based on data only for $3.0 \leq r_s \leq 6.2$ nm, the values of either hindrance factor outside that range represent extrapolations.

DISCUSSION

In the intact glomerular capillary wall, the GBM is interposed between two layers of cells, and an important issue is its relative contribution to the overall size selectivity of the barrier. This was assessed by comparing the present results with Ficoll sieving data obtained in vivo, as shown in Fig. 4. The in vivo data shown are the results reported by Oliver et al. (1992) for normal Munich-Wistar rats. Included for comparison are two curves based on the present results. The one marked "GBM" is the Ficoll sieving curve measured for $\Delta P = 35$ mmHg, which is close to the mean pressure obtained by Oliver et al. (1992) by micropuncture methods (34 mmHg). The second curve based on the present results, labeled "GBM (adjusted)," corrects for the differences in volume flux between the present experiments and those in vivo. As discussed in connection with Eqs. 3 and 4, there is an inverse relationship between the membrane Peclet number and the sieving coefficient, so that a more appropriate comparison between the in vivo and in vitro results is made on the basis of the same values of $\nu\delta$, the product that appears in the numerator of Eq. 4. The average value of ν in vivo was estimated as the single nephron glomerular filtration rate reported by Oliver et al. (1992), 49.8 nl/min, divided by a typical value for the glomerular surface area available for filtration, 0.002 cm^2 (Maddox et al., 1992); the result was $\nu = 4.2 \times 10^{-6}$ m/s. The thickness of one layer of GBM was estimated as 200 nm (Daniels et al., 1992), yielding $\nu\delta = 8.3 \times 10^{-13}$ m^2/s in vivo versus $\nu\delta = 4.5 \times 10^{-12}$ m^2/s in vitro at 35 mmHg (Table 1). Thus our experimental curve for GBM at 35 mmHg was adjusted to the in vivo estimate of $\nu\delta$ by using Eq. 3, resulting in an upward shift.

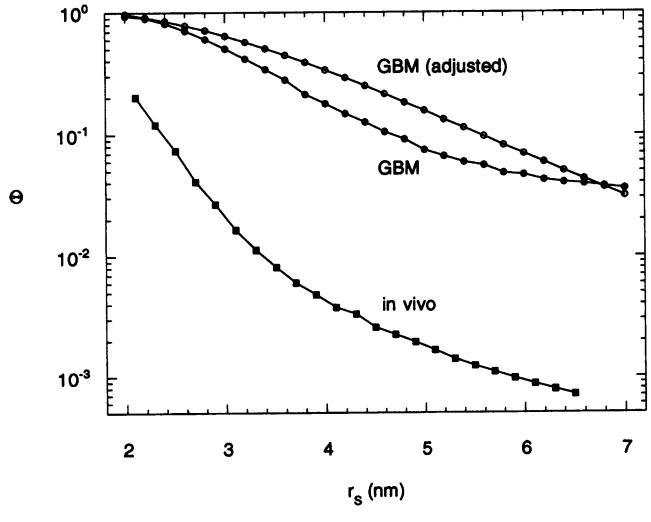

FIGURE 4 Comparison of Ficoll sieving coefficients in vitro and in vivo. The "in vivo" curve is based on the fractional clearance data of Oliver et al. (1992) in normal rats; the GBM curve represents the present results at $\Delta P = 35$ mmHg; the GBM (adjusted) curve is based on the volume flux and GBM thickness estimated for the rat in vivo (see text).

As shown in Fig. 4, either of the in vitro sieving curves lies well above that reported in vivo. Similar trends were reported previously using dextran (Daniels et al., 1993). To compare the contributions of the GBM and cell layers in a more quantitative manner, we note that for series barriers in general, the overall sieving coefficient is the product of the sieving coefficients for the individual layers. Accordingly, we assumed that the overall sieving coefficient in vivo (Θ_{wall}) equaled that for the cells (Θ_{cell}, corresponding to the endothelium and epithelium lumped together) times that for the GBM (Θ_{GBM}). Using the adjusted in vitro values as the estimates for Θ_{GBM} and the values of Oliver et al. (1992) for Θ_{wall}, we calculated $\Theta_{cell} = \Theta_{wall}/\Theta_{GBM} = (0.074)/(0.944) = 0.078$ at $r_s = 2.5$ nm and $\Theta_{cell} = (7.1 \times 10^{-4})/(5.8 \times 10^{-2}) = 1.2 \times 10^{-2}$ at $r_s = 6.5$ nm. It appears then that the cells are the dominant size-selective barrier, but that the contribution of the GBM is not negligible. Indeed, for the largest Ficoll ($r_s = 6.5$ nm), the sieving coefficient for the GBM is estimated to be of the same order of magnitude as that for the cell layers.

Another comparison of interest is between Ficoll and the more commonly used test macromolecule, dextran. It has been found previously that, for any given value of r_s, transmembrane movement of Ficoll is more hindered than that of dextran for diffusion in synthetic membranes (Davidson and Deen, 1988) and for glomerular filtration in the rat (Oliver et al., 1992). To compare the present results for Ficoll with those reported for similar experiments using dextran (Daniels et al., 1993), some interpolation and extrapolation was required. Because the experiments with dextran were performed at $\Delta P = 50$ mmHg, the present results at 35 mmHg and 60 mmHg were interpolated using Eqs. 3 and 8–10 to estimate the Ficoll curve at that pressure. Moreover, for the reasons discussed above, the adjusted Ficoll curve was calculated using the values of ν and δ reported in the dextran study. It was found that the sieving coefficients were lower with Ficoll than with dextran throughout the entire size range, by amounts ranging from 6% to 50%. This is qualitatively consistent with the trend noted previously with synthetic membranes and in vivo. However, these comparisons should be viewed with some caution, because the Darcy permeability was not measured in the dextran study. Thus the GBM filters might have had somewhat different properties.

A number of theories have been proposed to predict hindrance coefficients for macromolecules in basement membranes, connective tissues, synthetic hydrogels, and related materials, by representing the tissue or gel as an array of randomly oriented fibers. Extensive efforts were made to interpret our diffusive and convective hindrance factors for Ficoll using those fiber-matrix theories. The theories were found to be largely unsuccessful in correlating our data for isolated GBM, so that only a brief summary is

presented below; additional details of the calculations and results are given in Edwards (1996).

In the fiber-matrix theories the membrane is characterized largely by two parameters, the fiber radius (r_f) and the volume fraction of fibers (ϕ). Reasonable ranges for both quantities were estimated from previous morphological studies. Based on transmission electron micrographs, Laurie et al. (1984) described "cords" and "rods" in the GBM with diameters ranging from 4 to 10 nm. Kubosawa and Kondo (1985) found in the lamina rarae externa and interna (the portions of the GBM adjacent to the cells) a three-dimensional, polygonal network, consisting of interconnected fibrils 6–8 nm in diameter. The size of the mesh defined by these fibrils was variable, but ranged mainly from 20 to 25 nm. The three-dimensional mesh-like structure of the lamina densa (the central portion of the GBM) was also visualized in situ by Takami et al. (1991), who reported fibrils of 6–10 nm diameter arranged as a polygonal network. The average long dimension of the space between the fibers was estimated as 16.8 ± 6.2 nm, and the short dimension was 12.0 ± 6.2 nm. Thus we assumed values of r_f ranging from 2 to 5 nm. The fiber volume fraction in basement membranes has been reported as 0.11–0.12 in mouse EHS tumors (Haskin et al., 1993) and 0.17–0.21 in Descemet's membrane (Krause, 1934; Dohlman and Bazals, 1955), but to our knowledge there are no reported values of ϕ in GBM. For our calculations with the fiber matrix theories we assumed that ϕ ranged between 0.10 and 0.50.

A theory for diffusion and convection in random fibrous networks was proposed by Curry and Michel (1980), based largely on results for Φ and K_d derived by Ogston et al. (Ogston, 1958; Ogston et al., 1973). The approach of Curry and Michel has been applied previously to GBM by Robinson, Walton, and their co-workers (Robinson and Walton, 1987, 1989; Walton et al., 1992). When we attempted to interpret our results for $(\Phi K_d)_0$ using the theory of Ogston et al., major discrepancies were evident. Even the best fits to the data, obtained for $r_f = 2$ nm and $\phi = 0.42$, overestimated $(\Phi K_d)_0$ by a factor of ~2 at $r_s = 2.0$ nm and underestimated it by a factor of ~400 at $r_s = 7.0$ nm. In other words, this theory for partitioning and diffusion predicted much too sharp a decline in $(\Phi K_d)_0$ with increasing solute size. In analyzing our sieving (combined convection and diffusion) data using the model of Curry and Michel (1980), as employed by Robinson and Walton (1989), we were also unable to identify constant values of r_f and ϕ that would predict the observed dependence on molecular size. The best-fit values of r_f varied by ±20% over the range of molecular sizes, increasing from 1.7 to 2.5 nm as molecular size increased. Robinson and Walton reported similar percentage variations in r_f based on their data (although their absolute values of r_f were roughly one-half ours). It should be emphasized that although 1.7–2.5 nm might seem to be a reasonably tight range, it implies very large discrepancies in the Darcy (or hydraulic) permeability. Because the Darcy permeability varies as r_f^2 (see below), a 20% variation in r_f implies a variation of more than 40% in κ. Of course, for a given membrane and pressure, κ should be a constant.

Based on diffusion data for various macromolecules in agarose gels, a more recent model for the diffusional hindrance coefficient in random fibrous media appears to be more satisfactory than other approaches for predicting K_d (Johnson et al., 1996). For comparisons with our experimental results for $(\Phi K_d)_0$, the values of K_d predicted by this theory were combined with values of Φ obtained from the partitioning theory of Ogston (1958). One input in this diffusion model is the Darcy permeability at zero applied pressure, for which we used the value 2.40 nm^2 (see Eq. 12). The best-fit parameters for Ficoll diffusion in the GBM were $r_f = 4$ nm and $\phi = 0.39$. Even accepting what seems to be an unrealistically large value of ϕ, the results were not very satisfactory. The measured $(\Phi K_d)_0$ was overpredicted by a factor of ~2 for $r_s = 2.0$ nm and underpredicted by a factor of ~3 for $r_s = 7.0$ nm. Thus, once again, the theory predicts too sharp a decline in the rate of diffusion with increasing molecular size. Evidence for too strong a dependence of K_d on r_s in this theory was seen also in the agarose study, especially at the highest gel concentration studied ($\phi = 0.07$). Thus the less satisfactory results obtained with GBM may in part reflect the fact that it is a denser network.

An examination of the Darcy permeability data offered a clue to what may be missing in the fiber-matrix models for hindered transport, when applied to GBM. Two approaches were used to analyze κ. The first was based on the assumption that the membrane consists of a single type of fiber with a uniform radius r_f. In this approach the dependence of κ on r_f and ϕ was assumed to follow the correlation given by Jackson and James (1986) for three-dimensional arrays of fibers,

$$\kappa = -\frac{3r_f^2}{20\phi}[\ln \phi + 0.931 + O((\ln \phi)^{-1})]. \quad (11)$$

In addition, the dependence of κ on pressure was assumed to be linear. Using the measured values at $\Delta P = 35$ and 60 mmHg, this assumption gives

$$\kappa = 2.404 - 0.0264\Delta P, \quad (12)$$

where κ is in nm^2 and ΔP is in mmHg. With a fiber radius of $r_f = 2$ nm, Eqs. 11 and 12 yield solid volume fractions of $\phi = 0.19$ at 0 mmHg, 0.23 at 35 mmHg, and 0.27 at 60 mmHg. The corresponding values with $r_f = 5$ nm are $\phi =$ 0.32, 0.34 and 0.36, respectively. Assuming that the fibers form a square or hexagonal array, we estimated that the average spacing between fiber surfaces should then be about 3–7 nm, a range of values that is much lower than the literature estimates discussed earlier. The spacing of 16 nm reported by Takami et al. (1991) corresponds to $\phi = 0.04$ with $r_f = 2$ nm and $\phi = 0.13$ with $r_f = 5$ nm, assuming a hexagonal fiber array. Thus the volume fraction or number density of fibers observed by electron microscopy is too low to explain the small Darcy permeability of GBM.

The second approach used to examine the Darcy permeability assumes that representing the GBM as a network of identical fibers with a uniform radius may be too simplified. Indeed, the main components of the GBM (type IV collagen, laminin, heparan sulfate proteoglycans, entactin, and fibronectin) vary in size and structure, and a more accurate picture of the membrane is that of a basic fiber meshwork to which a variety of other polymers are linked, as described by Yurchenko and O'Rear (1993). The actual structure of the matrix might be more closely approximated if the GBM were treated as a composite fibrous medium with, say, two different types of fibers. Thus, in the second approach, the GBM was idealized as a random array of coarse fibers (radius a_c, volume fraction ϕ_c) embedded in a matrix of fine fibers (radius a_f, volume fraction ϕ_f).

Ethier (1991) developed a model for flow through a composite fibrous material composed of two types of fibers with significantly different radii. In this analysis the disparity in sizes has to be such that the fine matrix appears homogeneous on the length scale of the coarse fibers. The overall Darcy permeability was calculated as a function of the volume fraction of the coarse fibers, the radius of the fine fibers, and the Darcy permeability of the fine matrix. Assuming $a_f = 0.4$ nm, the value inferred by Ogston et al. (1973) for hyaluronic acid based on partitioning experiments, and $a_c = 2$–5 nm, as suggested above, we computed the overall Darcy permeability of the matrix as a function of ϕ_c. This was done using the zero shear model of Ethier (1991, equations 22, 40, and 46). We then related ϕ_c to the spacing between the coarse fibers, assuming that the latter formed a hexagonal array. Three different values of the total solid volume fraction ($\phi_t = \phi_c + \phi_f$) were considered, and the permeability of the fine matrix was calculated using Eq. 11.

The Darcy permeability results for the composite fiber matrix are shown in Fig. 5. Values of κ are shown as a function of the coarse fiber spacing, with the solid curves corresponding to the three values of ϕ_t. For this plot the radius of the coarse fibers was fixed at 4 nm. For any given valure of ϕ_t, it was found that κ decreased in a hyperbolic manner as the coarse-fiber spacing was increased (i.e., as ϕ_c was reduced). That is, as more and more of a fixed amount of solid was attributed to the fine fibers, there was a progressive decrease in the Darcy permeability. For a fixed coarse-fiber spacing (i.e., a fixed ϕ_c), the smaller the total solid volume fraction, the larger the overall permeability of the matrix. Essentially, in this model the Darcy permeability is governed mainly by the population of small fibers. Qualitatively similar results were obtained for other coarse fiber radii in the range of 2–5 nm.

Also shown in Fig. 5 (as *dashed lines*) are the values of the Darcy permeability for the GBM, including those measured at $\Delta P = 35$ and 60 mmHg and that extrapolated to $\Delta P = 0$. If we assume a certain value for the total solid volume fraction of the GBM, the coarse-fiber spacing can be determined from the corresponding curve. For example, if we postulate that $\phi_t = 0.15$, the coarse-fiber volume fraction for $\Delta P = 0$ is equal to 0.13 and the corresponding fiber spacing is 13 nm. With $\phi_t = 0.10$, $\phi_c = 0.08$ and the computed spacings are about 19 nm. These spacings are consistent with the aforementioned results from electron microscopy, if it is assumed that only the coarse fibers exhibited enough contrast to be visible. Thus the two-fiber model seems capable of reconciling the functional and morphological characteristics of the GBM. A more detailed model for water flow through a heterogeneous fiber matrix, including proteoglycan and collagen components, is that of Huang et al. (1994). Unfortunately, no heterogeneous fiber model is currently available for solute transport, and additional theoretical and experimental studies are needed if this concept is to be extended to macromolecular sieving.

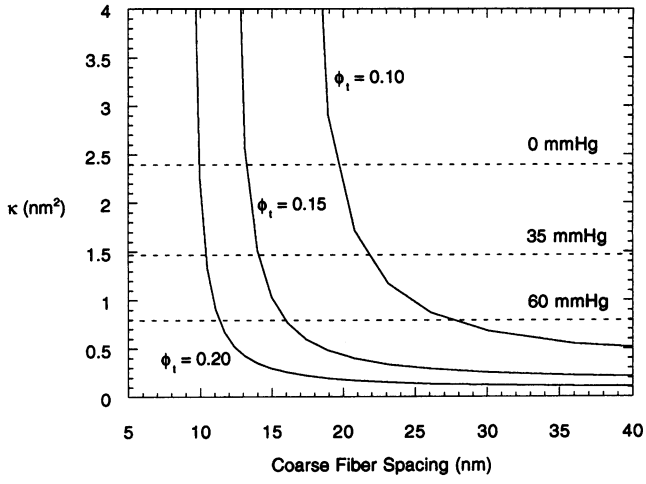

FIGURE 5 Darcy permeability (κ) as a function of the spacing between coarse fibers, for a material consisting of a mixture of coarse and fine fibers. Each curve corresponds to a fixed total volume fraction of fibers (ϕ_t), with fine and coarse fiber radii of 0.4 and 4 nm, respectively. The dashed lines indicate the values of κ measured (or estimated) for the GBM at three pressures.

In summary, the sieving data obtained with Ficoll showed that the contribution of the GBM to the overall size selectivity of the glomerular capillary wall is smaller than that of the cell layers, but is not negligible. The hydraulic permeabililty of the GBM was found to decrease with increasing pressure, suggesting that the permeability properties for macromolecules are also pressure dependent. The Ficoll results could be explained by assuming that the hindrance factors for diffusion and convection declined in a linear manner with increasing ΔP. Empirical expressions were derived to describe the dependence of the hindrance coefficients on molecular size and ΔP. The water permeability data for isolated GBM are consistent with a model in which the GBM is represented as a random fibrous network with two distinct populations of fibers.

APPENDIX

The sieving coefficient measured in any ultrafiltration study is affected by the extent of concentration polarization, which is governed by the mass

transfer coefficient in the retentate (k_c); the relationship is given in Eq. 7. Whereas the general behavior of k_c at the base of a stirred cylindrical cell is well understood (Colton and Smith, 1972), k_c depends on geometric factors such as impeller shape and location in a manner that is difficult to predict with precision. For this reason we elected to measure the mass transfer coefficient in a filtration cell identical to that used in the experiments with GBM. The approach used was to measure filtration rates across synthetic membranes with and without BSA in the retentate. The reduction in filtrate velocity due to osmotic pressure was related to the BSA concentration next to the membrane, allowing k_c to be computed for BSA. Extrapolation of this result to Ficoll of various sizes was straightforward, requiring mainly a correction for the different values of D_∞.

The mass transfer measurements were performed using a 25-mm-diameter ultrafiltration cell (model 3; Amicon Corporation, Danvers, MA). Applied pressures ranging from 25 to 75 mmHg were generated with compressed nitrogen and measured by a pressure transducer (model DP15; Validyne Engineering, Northridge, CA). The stirrer, calibrated using a strobe, was set at 220 rpm. Filtration rates were measured at room temperature (21°C) using 10,000-MW cutoff cellulose membranes (Millipore, Bedford, MA), which permitted <3% albumin passage. Three experimental periods were employed, each of which involved the collection of filtrate for 10 min after a 10-min equilibration time, during which the filtrate was discarded. The mass of filtrate (typically ~0.05 g) was determined using a digital balance. The initial volume of retentate in each period was 3 ml. In the first period the solution used was 0.15 M NaCl at pH 7.4. The cell was then rinsed and filled with a similar solution containing 4 g/dl BSA (Sigma). The retentate was sampled at the beginning and end of this second collection period for determination of the BSA concentration in the bulk retentate. The BSA concentrations in the retentate and filtrate were measured by absorbance at 280 nm. The third period was a repeat of the first. A given set of data was considered to be satisfactory only if the hydraulic permeability determined in the third period differed by <5% from that in the first.

The hydraulic permeability of the membrane was calculated from the data in the first and third periods (when BSA was absent) as $L_P = \nu/\Delta P$. Assuming that L_P remained the same with BSA present, the data in the second period yielded the value of $(1 - \Theta_{BSA})P_{BSA}$; see Eq. 5). To determine the albumin concentration at the upstream surface of the membrane, we used the semiempirical correlation developed by Vilker et al. (1981),

$$\Pi_{BSA} = RT\left\{2\left[\left(\frac{zC_{BSA}}{2M_{BSA}}\right)^2 + m_s^2\right]^{1/2} - 2m_s\right\} + \frac{RT}{M_{BSA}}(C_{BSA} + A_2C_{BSA}^2 + A_3C_{BSA}^3), \quad \text{(A1)}$$

where M_{BSA} is the molecular weight of albumin, C_{BSA} its concentration in g/l, z the charge number, R the gas constant, T the absolute temperature, and m_s the molar salt concentration. For 0.15 M NaCl at pH = 7.4, we have $z = -20.4$, $A_2 = -1.089 \times 10^{-2}$, and $A_3 = 1.243 \times 10^{-4}$. The quantities $\Delta\Pi_{BSA}$ and Θ_{BSA} were calculated by solving Eqs. 5 and A1 simultaneously using an iterative procedure; the initial guess for Θ_{BSA} was the BSA concentration in the filtrate divided by that in the bulk retentate. This allowed calculation of the BSA concentration at the membrane surface. Rearranging Eq. 7, the mass transfer coefficient was calculated as

$$k_c = \nu\left[\ln\left(\frac{C_M - C_F}{C_R - C_F}\right)\right]^{-1}, \quad \text{(A2)}$$

where C_M, C_R, and C_F are the BSA concentrations at the membrane surface, in the bulk retentate, and in the filtrate, respectively.

For filtrate velocities averaging 1.20×10^{-6} m/s, which were comparable to those in the experiments with GBM, the mass transfer coefficient for BSA at 21°C was found to be $k_c = (2.00 \pm 0.05) \times 10^{-6}$ m/s ($n = 16$), at 21°C. This result was extrapolated to 27°C (the temperature for the GBM studies) and to the various sizes of Ficoll by assuming that $k_c \propto \mu^{1/6}D_\infty^{2/3}$ (Colton and Smith, 1972), where μ is the viscosity of water. For BSA at 27°C the result was $k_c = 2.28 \times 10^{-6}$ m/s. This is significantly lower than the value predicted for these conditions by equation 5 of Colton and Smith (1972), which is 4.34×10^{-6} m/s.

Excellent technical assistance was provided by Michael Ahlquist, and help with the preparation of fluorescein-Ficoll was provided by Dr. Erin M. Johnson.

This work was supported by grants from the National Institutes of Health (DK20368 and DK45058). BD is the recipient of an American Heart Association Established Investigatorship.

REFERENCES

Colton, C. K., and K. A. Smith. 1972. Mass transfer to a rotating fluid. II. Transport from the base of an agitated cylindrical tank. *AIChE J.* 18:958–967.

Curry, F. E., and C. C. Michel. 1980. A fiber matrix model of capillary permeability. *Microvasc. Res.* 20:96–99.

Daniels, B. S. 1994. Determinants of charge selectivity of the glomerular permeability barrier. *J. Lab. Clin. Med.* 124:224–230.

Daniels, B. S., E. H. Hauser, W. M. Deen, and T. H. Hostetter. 1992. Glomerular basement membrane: in vitro studies of water and protein permeability. *Am. J. Physiol.* 262:F919–F926.

Daniels, B. S., W. M. Deen, G. Mayer, T. Meyer, and T. H. Hostetter. 1993. Glomerular permeability barrier in the rat: functional assessment by in vitro methods. *J. Clin. Invest.* 92:929–936.

Davidson, M. G., and W. M. Deen. 1988. Hindered diffusion of water-soluble macromolecules in membranes. *Macromolecules* 21:3474–3481.

De Belder, A. N., and K. Granath. 1973. Preparation and properties of fluorescein-labelled dextran. *Carbohydrate Res.* 30:375–378.

Dohlman, C. H., and E. A. Bazals. 1955. Descemet's membrane of the bovine cornea. *Arch. Biochem. Biophys.* 57:445.

Edwards, A. 1996. Filtration of macromolecules by renal glomerular capillaries. Ph.D. thesis. Massachusetts Institute of Technology.

Edwards, A., W. M. Deen, and B. S. Daniels. 1997. Hindered transport of macromolecules in isolated glomeruli. I. Diffusion across intact and cell-free capillaries. *Biophys. J.* 72:000–000.

Ethier, C. R. 1991. Flow through mixed fibrous porous materials. *AIChE J.* 37:1227–1236.

Haskin, C. L., I. L. Cameron, and D. H. Rohrbach. 1993. Role of water hydration on the filtration function of proteoglycans. *In* Molecular and Cellular Aspects of Basement Membranes. D. Rohrbach and R. Timpl, editors. Academic Press, New York. 89–106.

Huang, Y., D. Rumschitzki, S. Chien, and S. Weinbaum. 1994. A fiber matrix model for the growth of macromolecular leakage spots in the arterial intima. *J. Biomech. Eng.* 116:430–445.

Jackson, G. W., and D. F. James. 1986. The permeability of fibrous porous media. *Can. J. Chem. Eng.* 64:364–374.

Johnson, E. M., D. A. Berk, R. K. Jain, and W. M. Deen. 1996. Hindered diffusion in agarose gels: test of effective medium model. *Biophys. J.* 70:1017–1026.

Krause, A. C. 1934. The Biochemistry of the Eye. Johns Hopkins University Press, Baltimore.

Kubosawa, H., and Y. Kondo. 1985. Ultrastructural organization of the glomerular basement membrane as revealed by a deep-etch replica method. *Cell Tissue Res.* 242:33–39.

Laurie, G. W., C. P. Leblond, S. Inoue, G. R. Martin, and A. Chung. 1984. Fine structure of the glomerular basement membrane and immunolocalization of five basement membrane components to the lamina densa (basal lamina) and its extensions in both glomeruli and tubules of the rat kidney. *Am. J. Anat.* 169:463–481.

Maddox, D. A., W. M. Deen, and B. M. Brenner. 1992. Glomerular filtration. *In* Handbook of Physiology. Renal Physiology, Sect. 8, Vol. 1. American Physiological Society, Bethesda, MD. 545–638.

Ogston, A. G. 1958. The spaces in a uniform random suspension of fibers. *Trans. Faraday Soc.* 54:1754–1757.

Ogston, A. G., B. N. Preston, and J. D. Wells. 1973. On the transport of compact particles through solutions of chain-polymers. *Proc. R. Soc. Lond. A.* 333:297–316.

Oliver, J. D., S. Anderson, J. L. Troy, B. M. Brenner, and W. M. Deen. 1992. Determination of glomerular size selectivity in the normal rat with Ficoll. *J. Am. Soc. Nephrol.* 3:214–228.

Robinson, G. B., and H. A. Walton. 1987. Ultrafiltration through basement membrane. *In* Renal Basement Membranes in Health and Disease. R. G. Price and B. G. Hudson, editors. Academic Press, London. 147–161.

Robinson, G. B., and H. A. Walton. 1989. Glomerular basement membrane as a compressible ultrafilter. *Microvasc. Res.* 38:36–48.

Takami, H., A. Naramoto, H. Shigematsu, and S. Ohno. 1991. Ultrastructure of glomerular basement membrane by quick-freeze and deep-etch methods. *Kidney Int.* 39:659–664.

Vilker, V. L., C. K. Colton, and K. A. Smith. 1981. The osmotic pressure of concentrated protein solutions: effect of concentration and pH in saline solutions of bovine serum albumin. *J. Colloid. Interface Sci.* 79:548–566.

Walton, H. A., J. Byrne, and G. B. Robinson. 1992. Studies of the permeation properties of glomerular basement membrane: cross-linking renders glomerular basement membrane permeable to protein. *Biochim. Biophys. Acta.* 1138:173–183.

Yurchenko, P. D., and J. O'Rear. 1993. Supramolecular organization of basement membranes. *In* Molecular and Cellular Aspects of Basement Membranes. D. Rohrbach and R. Timpl, editors. Academic Press, New York. 19–47.